

## Topological Swing of Bloch Oscillations in Quantum Walks

Lavi K. Upreti<sup>1</sup>, C. Evain<sup>2</sup>, S. Randoux<sup>2</sup>, P. Suret<sup>2</sup>, A. Amo<sup>2</sup>, and P. Delplace<sup>1</sup>

<sup>1</sup>*Université Lyon, ENS de Lyon, Université Claude Bernard, CNRS, Laboratoire de Physique, F-69342 Lyon, France*

<sup>2</sup>*Université Lille, CNRS, UMR 8523—PhLAM—Physique des Lasers Atomes et Molécules, F-59000 Lille, France*



(Received 30 April 2020; accepted 23 September 2020; published 30 October 2020)

We report new oscillations of wave packets in quantum walks subjected to electric fields, that decorate the usual Bloch-Zener oscillations of insulators. The number of turning points (or suboscillations) within one Bloch period of these oscillations is found to be governed by the winding of the quasienergy spectrum. Thus, this provides a new physical manifestation of a topological property of periodically driven systems that can be probed experimentally. Our model, based on an oriented scattering network, is readily implementable in photonic and cold atomic setups.

DOI: [10.1103/PhysRevLett.125.186804](https://doi.org/10.1103/PhysRevLett.125.186804)

Periodically driven systems are routinely used to engineer artificial gauge fields and induce exotic topological properties. A remarkable case is the so-called anomalous topological boundary modes, which have no counterpart at equilibrium and were predicted [1] and observed in experimental platforms as different as photonics, cold atoms, and acoustics [2–10]. The existence of these states actually follows from the periodicity of the quasienergy spectrum that is itself inherited from the periodic drive.

Beyond these anomalous edge states, the frequency periodicity also allows the quasienergy spectrum to wind, which constitutes a distinct, so far largely overlooked topological property of the bands specific to periodically driven systems [11–13]. One of the main consequences of this winding is the modification of the wave packet dynamics in the bulk of the system. The celebrated Thouless pumping, which consists of a quantized mean displacement of a particle in a 1D lattice subject to an adiabatic periodic drive [14], was originally understood in terms of Berry curvature and was later rephrased as a winding property of the quasienergy spectrum with respect to the quasimomentum [13,15]. Indeed, the measurement of wave packet dynamics constitute one of the very few tools to probe geometrical and topological band properties of insulators. The associated anomalous velocity induces a measurable drift of the wave packet that gives experimental access to the Berry curvature of the bulk bands [16]. This geometrical information was measured in periodically driven systems such as shaken trapped cold atoms gases [17], photonic quantum walks [18], and in nonperiodic structures [19].

Here we report a new topological property of the motion of wave packets that appears in periodically driven systems containing bands with a nontrivial winding. While previous studies take advantage of usual Bloch oscillations to probe the lateral drifts associated to nontrivial Berry curvature

[20–24] or Berry-Zak phases of the bands [25–28], we find that periodically driven systems may exhibit a whole family of new Bloch-like oscillations with nontrivial properties. Differently from kicked rotors in which Bloch-like oscillations have been observed [29,30], the oscillatory phenomenon we unveil is directly related to the topology of the bands. To explore this physics we propose a model of a 1D quantum walk with a time-varying synthetic electric field that is realizable in current photonic setups, and we find that the winding number characterizing the bands governs the number of suboscillations of a wave packet within a Bloch-Zener period. This topological feature guarantees the robustness of the number of these additional suboscillations irrespective of the coupling parameters of the model that, instead, determine their amplitude and shape. Finally, we discuss a parallel between these oscillations and Thouless pumping as they both reflect two complementary topological aspects of wave packet dynamics that can be expressed in terms of distinct winding numbers of the quasienergy spectrum.

The model we consider is sketched in Fig. 1. It consists of an oriented scattering network that represents a discrete-time evolution of a quantum state or a wave packet through a periodic succession of scattering nodes (from top to bottom). The discrete-time periodic dynamics are abundantly used in topological physics, both theoretically, where they were first introduced to illustrate the anomalous edge states [1,13,31–36], and experimentally in classical photonics [4–6,37], in a quantum optics context [38–40], and in cold atomic setups [41,42], where they are often referred to as discrete-time quantum walks [41,43,44]. The scattering network in Fig. 1 is a representation of such 1D quantum walks. It has the advantage to be particularly suitable for a photonic interpretation, as the nodes simply describe beam splitters and the oriented links represent the free propagation of a light pulse with time. It describes previous experiments, e.g., in 1D split-step quantum

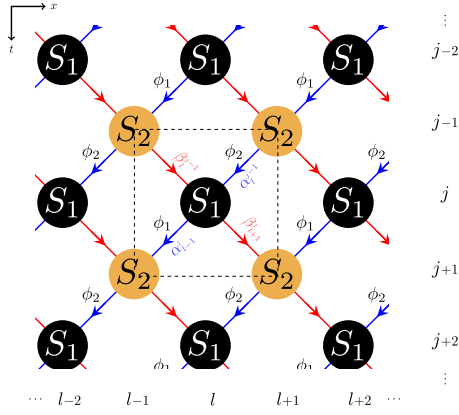


FIG. 1. Two-steps oriented scattering network, where an input signal flows from top to bottom. Black and orange nodes represent two distinct scattering processes that repeat periodically. Two staggered phase shifts,  $\phi_1$  and  $\phi_2$ , are also considered along the leftward paths. A dashed square emphasizes the unit cell of this lattice.

walks [38], planar periodically coupled waveguides [6] and coupled fiber rings [18,45]. In the following, we shall thus stick to this scattering network picture to model our periodic discrete-time evolution, but an equivalent Hamiltonian formalism is provided in Ref. [46].

The network depicts a succession of two scattering events occurring at time steps  $j$  and positions  $l$ , between incoming leftward and rightward wave amplitudes  $\alpha_l^{j-1}$  and  $\beta_l^{j-1}$ , toward leftward and rightward outgoing states  $\alpha_{l-1}^j$  and  $\beta_{l+1}^j$ . These scattering amplitudes are encoded in a dimensionless parameter  $\theta_j$  entering the unitary matrix

$$S_j = \begin{pmatrix} \cos \theta_j & i \sin \theta_j \\ i \sin \theta_j & \cos \theta_j \end{pmatrix}. \quad (1)$$

For simplicity, we consider only two distinct beam splitters,  $S_1$  and  $S_2$ , per time period, but the model can be generalized to further scattering events. Besides, we introduce a phase shift carried by the waves along their free propagation between these beam splitters, as in Ref. [18]. Without any loss of generality, we consider a nonzero phase shift for the leftward states only (in blue in Fig. 1). It was shown previously that such a phase induces a synthetic electric field when slowly varied in time over many periods [47]. A crucial point of the model is that this phase shift takes two different values  $\phi_1 \neq \phi_2$  after each of the two scattering events ( $S_1$  and  $S_2$ ) within a period of the quantum walk. The ratio of these phases is chosen to be a rational number, and we set  $\phi_1 = (m_1/n_1)\phi$  and  $\phi_2 = (m_2/n_2)\phi$  with  $m_j, n_j \in \mathbb{Z}$ . As a result, the phase shift follows two time scales: a short one, that is the two-step period of the photonic quantum walk (called Floquet period in the following), and which is fixed by the values of  $m_j$  and  $n_j$ ; and a much longer one over which  $\phi$  may be adiabatically varied, in order to generate a fictitious electric

field. The rapid variations of the phase within a Floquet period allow the generation of electric fields specific to periodically driven systems when  $\phi$  is adiabatically varied. As we shall see, this gives rise to an original topological property of the evolution operator that manifests through unusual topological Bloch oscillations.

The time evolution of a state in the scattering network is given by relating the outgoing scattering amplitudes at time step  $j$  to that at time step  $j-1$ , according to the scattering parameters Eq. (1)

$$\begin{aligned} \alpha_{l-1}^j &= (\cos \theta_j \alpha_l^{j-1} + i \sin \theta_j \beta_l^{j-1}) e^{i\phi_j} \\ \beta_{l+1}^j &= i \sin \theta_j \alpha_l^{j-1} + \cos \theta_j \beta_l^{j-1}. \end{aligned} \quad (2)$$

where  $\tilde{j} = \text{mod}[j, 2]$ . Assuming discrete translation invariance along the  $x$  direction, the system can be treated in the Bloch-Floquet formalism. The corresponding Floquet unitary evolution operator  $U_F(k, \phi)$  after a periodic sequence of two steps readily describes a succession of local scattering events  $S_j$  followed by rightward and leftward translations  $T_j$ :

$$U_F(k, \phi_1, \phi_2) = e^{i(\phi_1 + \phi_2)/2} T_2 S_2 T_1 S_1 \quad (3)$$

$$T_j = \begin{pmatrix} e^{i(k - \phi_j/2)} & 0 \\ 0 & e^{-i(k - \phi_j/2)} \end{pmatrix} \quad (4)$$

where  $k$  is the dimensionless quasimomentum in the  $x$  direction, and we have removed the tilde from the  $j$  for the sake of clarity. Importantly, this quasimomentum is shifted by a phase  $\phi_j$  that can thus be interpreted as a time-step dependent vector potential. Since the Floquet operator  $U_F(k, \phi)$  depends periodically on the two variables  $k$  and  $\phi$ , one can introduce a synthetic 2D Brillouin zone (BZ) to describe its eigenvalues spectrum. They decompose as  $\lambda = e^{i\epsilon}$ , where  $\epsilon$  are hereafter referred to as the dimensionless quasienergy.

The global phase factor in Eq. (3) suggests that a peculiar spectral property arises when imposing a net phase  $\phi_1 + \phi_2 \neq 0$  per period. In that case, the generalized inversion symmetry  $U_F(-k, -\phi) = \sigma_x U_F(k, \phi) \sigma_x$  (with  $\sigma_x$  the standard Pauli matrix) is broken [46], leading to a winding of the quasienergy bands when  $\phi$  is varied, as illustrated in Fig. 2(a). A similar quasienergy winding was reported when considering periodically driven trapped cold atoms with a different protocol [15].

The period  $\Phi$  of the BZ along  $\phi$  [i.e.,  $\epsilon(k, \phi + \Phi) = \epsilon(k, \phi)$ ] depends on  $m_j$  and  $n_j$  as  $\Phi = 4\pi \text{LCM}[(m_1/n_1 - m_2/n_2)^{-1}, (m_1/n_1 + m_2/n_2)^{-1}]$ , where LCM indicates the least common multiple [46]. This allows us to define the winding of the quasienergies along  $\phi$  as

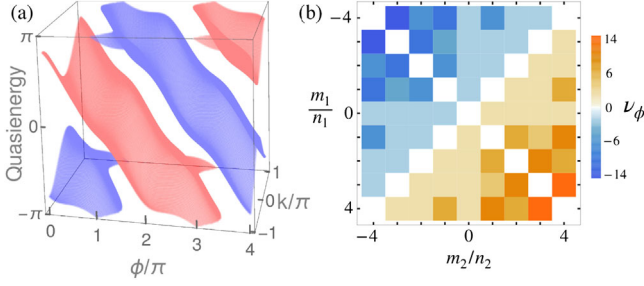


FIG. 2. (a) Quasienergy spectrum with a winding  $\nu_\phi = -2$  obtained for a scattering model with two steps per period for  $\theta_1 = \pi/4$ ,  $\theta_2 = \pi/4 - 0.6$ ,  $\phi_1 = \phi$  and  $\phi_2 = -2\phi$ . (b) Values of  $\nu_\phi$  for integer values of  $m_j/n_j$ .

$$\nu_\phi \equiv \sum_{p=1}^N \frac{1}{2\pi} \int_0^\Phi d\phi \frac{\partial \varepsilon_p(k, \phi)}{\partial \phi} = \frac{1}{2\pi i} \int_0^\Phi d\phi \text{tr}[U_F^{-1} \partial_\phi U_F]. \quad (5)$$

This winding number is a topological property of the Floquet evolution operator, as it reads as an element of the homotopy group  $\pi_1[U(N)] = \mathbb{Z}$ . Note that  $\nu_\phi$  is an even integer in our specific case due to the even number of bands ( $N = 2$ ) in our model. A direct calculation leads to the simple result

$$\nu_\phi = \frac{\Phi}{2\pi} \left( \frac{m_1}{n_1} + \frac{m_2}{n_2} \right), \quad (6)$$

which remarkably does not depend either on  $k$  (since the winding of a quasienergy band  $\varepsilon_p(k, \phi)$  along  $\phi$  must be the same for any  $k$ ) or on the scattering amplitudes  $\theta_j$ .

Instead, it is proportional to the net phase  $(\phi_1 + \phi_2)/\phi$  that breaks inversion symmetry. A phase diagram representing the different possible values of  $\nu_\phi$  as a function of  $m_j/n_j$  is shown in Fig. 2(b).

A striking consequence of the winding of the quasienergy bands is the unconventional dynamics of the wave packets in position space when adiabatically increasing the coordinate  $\phi$ . In the following, we show how these dynamics reveal a new kind of Bloch oscillations described by the winding number  $\nu_\phi$ . Figure 3(b) shows the  $j$ -time evolution of a Gaussian wave packet injected at  $j = 0$  in the blue band of Fig. 2(a) at  $k = 0$ , when  $\phi$  is adiabatically increased from 0 to  $\Phi = 4\pi$ , with  $\phi(j) = \gamma_0 j$  where the rate  $\gamma_0 = 2\pi/2000$  [see Fig. 3(a)]. To compute the spatio-temporal dynamics, we apply Eq. (2) to the initial wave packet. The wave packet periodically oscillates in the space coordinate while keeping  $k$  constant. This can be readily seen in Figs. 3(c)–3(f), where we show the 2D Fourier transform of the wave packet after having evolved to the time step indicated by the horizontal lines in Fig. 3(b). These panels provide a phenomenological understanding of the mechanism behind the oscillations: as  $\phi$  is adiabatically increased, the band dispersions are displaced in a diagonal direction in  $(k, \varepsilon)$  space [green arrows in Figs. 3(c)–3(f)], a direct consequence of the winding of the bands [see also Fig. 2(a)]. Therefore, the group velocity  $v_g = \partial \varepsilon / \partial k$  of a wave packet with a given  $k$  changes sign when  $\phi(j)$  increases, resulting in oscillations in the spatial coordinate.

It is worth stressing that two distinct drivings are present in our model: (i) a fast cyclic driving of the phases  $\phi_1, \phi_2$  within a Floquet period, which confers a nontrivial winding to the bands; (ii) a slow adiabatic increase of the phase  $\phi$

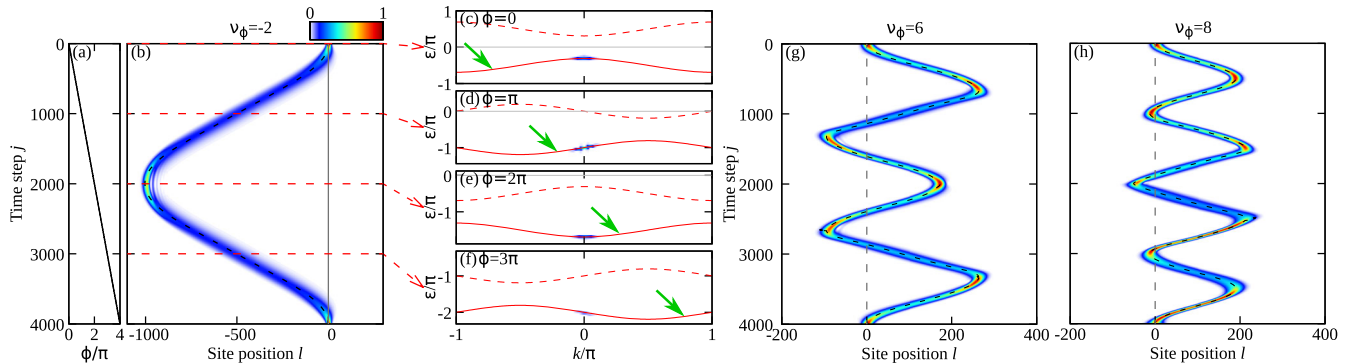


FIG. 3. (a) Adiabatic increase of  $\phi$  leads to (b) a standard Bloch oscillation ( $\nu_\phi = -2$ ), and (g),(h) Bloch oscillation with subs oscillations ( $\nu_\phi = 6$  and  $\nu_\phi = 8$ , respectively) of a wave packet injected at time  $j = 0$  and position  $l = 0$  with a Gaussian shape with rms width of 10 sites in one band [the blue band in Fig. 2(a) for the case of (b)]. Color scale: intensity of the wave packet ( $|\alpha_l^j|^2 + |\beta_l^j|^2$ ). Dashed black line: analytical calculation of the centre of mass motion of a wave packet from Eq. (32) in [46]. (b),(g),(h) show one period  $T_B$  of oscillation for the values of  $(m_1, m_2, n_1, n_2), \theta_1, \theta_2$  as  $(1, -2, 1, 1), \pi/4, \pi/4 - 0.5$  for (b);  $(4, -1, 1, 1), \pi/4, \pi/4 - 0.2$  for (g); and  $(9, -1, 2, 2), \pi/4, \pi/4 - 0.2$  for (h). In (c)–(f), the norm of the 2D Fourier transform of the wave packet ( $\alpha$  part) after having evolved to the time step indicated by the horizontal lines in (b), and both the solid and the dashed red lines represent numerically calculated bands [Eq. (33) in Ref. [46]]. The vertical scales differ in each panel. The green arrows show the direction in which the bands wind when  $\phi$  increases.

which results in the oscillations. An analytical calculation of the center of mass trajectory  $X_c(t, k)$  of the wave packet initially injected at a given  $k$  can be inferred from the group velocity of the quasienergy bands in parameter space [46]:

$$X_c(t, k) = \gamma_0 \int_0^t d\tau v_g(\phi(\tau), k), \quad (7)$$

where the continuous-time variable  $t$  extrapolates the discrete one  $j$ . This semiclassical trajectory is shown in black dashed lines in Fig. 3(b), which fits the simulation plot perfectly.

More importantly, the observed oscillatory phenomenon establishes a direct connection between the winding of the bands in our Floquet-Bloch model and the usual Bloch oscillations in a periodic crystal subject to a constant electric field. Indeed, the adiabatic increase of the phase shift  $\phi$  at a rate  $\gamma_0$  when the time steps  $j$  increase is analogous to a time-dependent vector potential that induces a (fictitious) electric field [48]  $E$  and, therefore, should result in Bloch oscillations. This was already noticed in the case of a single-step time evolution by Wimmer and co-workers [49], who reported a gauge transformation relating the dynamics of a wave packet in a lattice subject to a static potential gradient (i.e., a constant electric field), and the dynamics in a lattice subject to an adiabatic increase of the parameter  $\phi$  (see also Ref. [46]).

To establish the connection between the winding of the quasienergy bands and Bloch oscillations, we note that the time periodicity  $T_B$  of the center of mass motion  $X_c$  is inherited from the periodicity of the quasienergy with respect to  $\phi$  in the following way:

$$T_B = \frac{2\pi}{\gamma_0} \frac{\nu_\phi}{\frac{m_1}{n_1} + \frac{m_2}{n_2}}, \quad (8)$$

where negative values of  $\nu_\phi$  correspond to mirror symmetric trajectories to those with  $|\nu_\phi|$ .

In Eq. (8), we recognize the usual period  $T_B$  for Bloch oscillations induced by an average constant electric field  $E = (E_1 + E_2)/2$  where  $E_j = (m_j/n_j)\gamma_0$  is the fictitious electric field applied during the time step  $j$  (see Ref. [46] for more details), except that in Eq. (8) this standard relation is modified by the winding number  $\nu_\phi$ . In particular, the period  $T_B = 2\pi/E$  of the usual Bloch oscillations is recovered for  $|\nu_\phi| = 2$ , a situation in which each band winds once, as reported in Figs. 2(a) and 3(b).

Beyond this standard case, our model predicts a novel kind of topological oscillations: higher winding numbers may not only change the period  $T_B$ , but also yield more complex oscillations with additional turning points within  $T_B$ . Two examples are shown in Figs. 3(g) and 3(h) for values of  $m_i, n_i$  resulting in bands of windings  $\nu_\phi = 6$  and 8, respectively, and the same oscillating period  $T_B$  as in

Fig. 3(b). Remarkably, in a period  $T_B$ , the number of turning points is found to be precisely  $\mathcal{N}_t = |\nu_\phi|$  (see Ref. [46]). This result confers a topological nature to the observed oscillations. Note that standard Bloch oscillations simply have two turning points per period [see Fig. 3(b)], in agreement with  $\mathcal{N}_t = 2 = |\nu_\phi|$ . Moreover, the topological nature of the oscillations makes them robust to the presence of weak disorder in the lattice [46].

So far, we have considered windings of the bands induced by periodic pumping in the synthetic dimension. We now show that a winding of the quasienergy bands along the  $k$  direction can similarly be induced when inversion symmetry is broken in the spatial dimension, and it results in a different topological phenomenon: quantized displacement of the mean particle position. This effect can be straightforwardly implemented in scattering network models by connecting next-nearest neighbor nodes, as sketched in Fig. 4(a) for a two-step time evolution (see Ref. [46] for the step evolution equations). For the sake of generality, we have kept in the model the phase  $\phi_j$ , which we take as  $\phi_1 = \phi = -\phi_2$ , such that  $\nu_\phi = 0$ , i.e., there are no Bloch oscillations. The corresponding quasienergy bands, displayed in Fig. 4(b), show a winding along  $k$  for each  $\phi$ . This feature is captured by a winding number of the Floquet operator along  $k$ , analogous to that defined in Eqs. (5) and (6) for  $\phi$ . More generally, when considering even further long range couplings, this winding number is found to read [46]

$$\nu_k = \frac{\kappa}{2\pi} \left( \frac{r_1}{s_1} + \frac{r_2}{s_2} \right) \quad (9)$$

where  $\kappa$  is the periodicity of the bands in  $k$  and  $r_j/s_j$  is related to the range of the couplings between nodes to the left or to the right at each time step  $j$ . For the case illustrated in Fig. 4(a),  $r_1/s_1 = 1$ ,  $r_2/s_2 = -2$ .

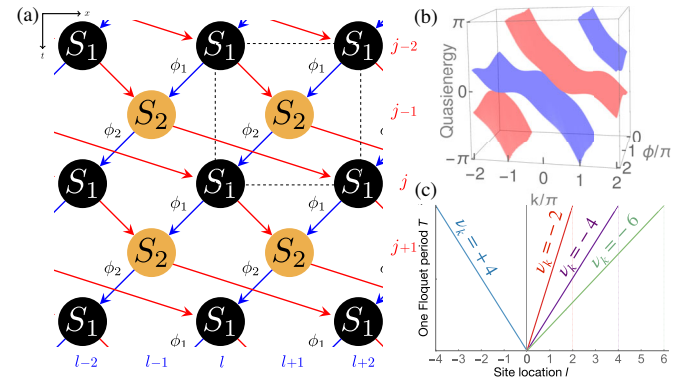


FIG. 4. (a) Two-steps scattering network with the next nearest coupling in the second step. A dashed black rectangle emphasizes the unit cell of this lattice. (b) Quasienergy bulk spectrum for the model depicted in (a) with  $\theta_1 = \pi/4$ ,  $\theta_2 = \pi/4 - 0.6$  and  $\phi_1 = -\phi_2$ . (c) Quantized displacement of the mean particle position with associated winding numbers  $\nu_k$ .

In the spirit of the seminal work of Thouless [14], and as revisited by Kitagawa *et al.* [13] within the Floquet formalism, this winding number  $\nu_k$  can be related to the mean displacement of particles after  $P$  Floquet periods  $T$ , in a state where all the bands are uniformly excited, that is Ref. [46], which also includes Ref. [50],  $\Delta x = -P(2\pi/\kappa)\nu_k$ .

Despite this apparent similarity, this quantized transport property differs from the usual Thouless pumping that results from an *adiabatic* driving of the system. In that case, the quantization can be expressed as a Chern number of the slowly driven instantaneous filled states parametrized over the effective 2D BZ  $(k, t)$ . This Chern number was later reinterpreted as a sum of the winding numbers in  $k$  over the filled bands [13]. In the adiabatic regime, if this sum runs over all the bands, as in our case, then the Chern numbers of each band sum up to zero, and there is no drift. Quantized drifts obtained for our *nonadiabatic* scattering model are shown in Fig. 4(c). More generally, quasienergy windings along both  $\phi$  and  $k$  coordinates can coexist, leading to quite complex drifted Bloch oscillations for wave packets, which are shown in Ref. [46].

Our study unveils the topological aspects of Bloch oscillations and extends them to a family of oscillatory phenomena accessible in artificial systems such as arrays of photonic waveguides and coupled fibers. It generalizes straightforwardly to periodically driven lattices of ultracold atoms where a protocol to generate quasienergy windings and oscillations was proposed [15], although neither the winding number  $\nu_\phi$  nor its relation to the number of Bloch suboscillations was identified. The direct relation we have identified between the number of turning points within an oscillation period and the winding number of the bands provides a new protocol to measure topological invariants in systems described by a quantum walk. The study of the manifestation of the topological nature of the oscillations in their associated Wannier-Stark ladders [51] remains an exciting perspective.

The authors are thankful to Benoit Douçot for his very constructive comments. This work was supported by the French Agence Nationale de la Recherche (ANR) under grant Topo-Dyn (ANR-14-ACHN-0031), the Labex CEMPI (ANR-11-LABX-0007), the CPER Photonics for Society P4S, the I-Site ULNE project NONTOP, the *Métropole Européenne de Lille* (project TFlight) and the European Research Council (ERC) under the European Unions Horizon 2020 research and innovation programme (Grant Agreement No. 865151).

- 
- [1] M. S. Rudner, N. H. Lindner, E. Berg, and M. Levin, *Phys. Rev. X* **3**, 031005 (2013).  
 [2] M. C. Rechtsman, J. M. Zeuner, Y. Plotnik, Y. Lumer, D. Podolsky, F. Dreisow, S. Nolte, M. Segev, and A. Szameit, *Nature (London)* **496**, 196 (2013).

- [3] F. Gao, Z. Gao, X. Shi, Z. Yang, X. Lin, H. Xu, J. D. Joannopoulos, M. Soljačić, H. Chen, L. Lu *et al.*, *Nat. Commun.* **7**, 11619 (2016).  
 [4] L. J. Maczewsky, J. M. Zeuner, S. Nolte, and A. Szameit, *Nat. Commun.* **8**, 13756 (2017).  
 [5] S. Mukherjee, A. Spracklen, M. Valiente, E. Andersson, P. Öhberg, N. Goldman, and R. R. Thomson, *Nat. Commun.* **8**, 13918 (2017).  
 [6] M. Bellec, C. Michel, H. Zhang, S. Tzortzakos, and P. Delplace, *Europhys. Lett.* **119**, 14003 (2017).  
 [7] S. Afzal, T. J. Zimmerling, Y. Ren, D. Perron, and V. Van, *Phys. Rev. Lett.* **124**, 253601 (2020).  
 [8] Y.-G. Peng, C.-Z. Qin, D.-G. Zhao, Y.-X. Shen, X.-Y. Xu, M. Bao, H. Jia, and X.-F. Zhu, *Nat. Commun.* **7**, 13368 (2016).  
 [9] R. Fleury, A. B. Khanikaev, and A. Alù, *Nat. Commun.* **7**, 11744 (2016).  
 [10] K. Wintersperger, C. Braun, F. N. Ünal, A. Eckardt, M. D. Liberto, N. Goldman, I. Bloch, and M. Aidelsburger, *Nat. Phys.* **16**, 1058 (2020).  
 [11] A. Tanaka and M. Miyamoto, *Phys. Rev. Lett.* **98**, 160407 (2007).  
 [12] M. Miyamoto and A. Tanaka, *Phys. Rev. A* **76**, 042115 (2007).  
 [13] T. Kitagawa, E. Berg, M. Rudner, and E. Demler, *Phys. Rev. B* **82**, 235114 (2010).  
 [14] D. J. Thouless, *Phys. Rev. B* **27**, 6083 (1983).  
 [15] L. Zhou, C. Chen, and J. Gong, *Phys. Rev. B* **94**, 075443 (2016).  
 [16] D. Xiao, M.-C. Chang, and Q. Niu, *Rev. Mod. Phys.* **82**, 1959 (2010).  
 [17] M. Aidelsburger, M. Lohse, C. Schweizer, M. Atala, J. T. Barreiro, S. Nascimbène, N. R. Cooper, I. Bloch, and N. Goldman, *Nat. Phys.* **11**, 162 (2015).  
 [18] M. Wimmer, H. M. Price, I. Carusotto, and U. Peschel, *Nat. Phys.* **13**, 545 (2017).  
 [19] Y. E. Kraus, Y. Lahini, Z. Ringel, M. Verbin, and O. Zeitler, *Phys. Rev. Lett.* **109**, 106402 (2012).  
 [20] S. Longhi, *Opt. Lett.* **32**, 2647 (2007).  
 [21] A. Szameit, F. Dreisow, M. Heinrich, R. Keil, S. Nolte, A. Tünnermann, and S. Longhi, *Phys. Rev. Lett.* **104**, 150403 (2010).  
 [22] M. Cominotti and I. Carusotto, *Europhys. Lett.* **103**, 10001 (2013).  
 [23] N. Fläschner, B. S. Rem, M. Tarnowski, D. Vogel, D.-S. Lühmann, K. Sengstock, and C. Weitenberg, *Science* **352**, 1091 (2016).  
 [24] T. Li, L. Duca, M. Reitter, F. Grusdt, E. Demler, M. Endres, M. Schleier-Smith, I. Bloch, and U. Schneider, *Science* **352**, 1094 (2016).  
 [25] M. Atala, M. Aidelsburger, J. T. Barreiro, D. Abanin, T. Kitagawa, E. Demler, and I. Bloch, *Nat. Phys.* **9**, 795 (2013).  
 [26] J. Höller and A. Alexandradinata, *Phys. Rev. B* **98**, 024310 (2018).  
 [27] D. N. Maksimov, E. N. Bulgakov, and A. R. Kolovsky, *Phys. Rev. A* **91**, 053631 (2015).  
 [28] A. R. Kolovsky, *Phys. Rev. A* **98**, 013603 (2018).  
 [29] J. Floß and I. S. Averbukh, *Phys. Rev. Lett.* **113**, 043002 (2014).

- [30] J. Floß, A. Kamalov, I. S. Averbukh, and P. H. Bucksbaum, *Phys. Rev. Lett.* **115**, 203002 (2015).
- [31] G. Q. Liang and Y. D. Chong, *Phys. Rev. Lett.* **110**, 203904 (2013).
- [32] M. Pasek and Y. D. Chong, *Phys. Rev. B* **89**, 075113 (2014).
- [33] C. Tauber and P. Delplace, *New J. Phys.* **17**, 115008 (2015).
- [34] P. Titum, E. Berg, M. S. Rudner, G. Refael, and N. H. Lindner, *Phys. Rev. X* **6**, 021013 (2016).
- [35] P. Delplace, M. Fruchart, and C. Tauber, *Phys. Rev. B* **95**, 205413 (2017).
- [36] P. Delplace, *SciPost Phys.* **8**, 081 (2020).
- [37] W. Hu, J. C. Pillay, K. Wu, M. Pasek, P. P. Shum, and Y. D. Chong, *Phys. Rev. X* **5**, 011012 (2015).
- [38] T. Kitagawa, M. A. Broome, A. Fedrizzi, M. S. Rudner, E. Berg, I. Kassal, A. Aspuru-Guzik, E. Demler, and A. G. White, *Nat. Commun.* **3**, 882 (2012).
- [39] A. D’Errico, F. Cardano, M. Maffei, A. Dauphin, R. Barboza, C. Esposito, B. Piccirillo, M. Lewenstein, P. Massignan, and L. Marrucci, *Optica* **7**, 108 (2020).
- [40] Y. Meng, F. Mei, G. Chen, and S. Jia, *Quantum Inf. Process.* **19**, 118 (2020).
- [41] T. Groh, S. Brakhane, W. Alt, D. Meschede, J. K. Asbóth, and A. Alberti, *Phys. Rev. A* **94**, 013620 (2016).
- [42] M. Sajid, J. K. Asboth, D. Meschede, R. Werner, and A. Alberti, *Phys. Rev. B* **99**, 214303 (2019).
- [43] T. Kitagawa, M. S. Rudner, E. Berg, and E. Demler, *Phys. Rev. A* **82**, 033429 (2010).
- [44] J. K. Asbóth and J. M. Edge, *Phys. Rev. A* **91**, 022324 (2015).
- [45] S. Weidemann, M. Kremer, T. Helbig, T. Hofmann, A. Stegmaier, M. Greiter, R. Thomale, and A. Szameit, *Science* **368**, 311 (2020).
- [46] See Supplemental Material at <http://link.aps.org/supplemental/10.1103/PhysRevLett.125.186804> which includes the proof of the connection between winding number  $\nu_\phi$  and stationary points in one Bloch period. Also, derivation of equivalent Hamiltonian formalism, and winding number and its connection with observable quantities.
- [47] A. Regensburger, C. Bersch, M.-A. Miri, G. Onishchukov, D. N. Christodoulides, and U. Peschel, *Nature (London)* **488**, 167 (2012).
- [48] J. B. Krieger and G. J. Iafrate, *Phys. Rev. B* **33**, 5494 (1986).
- [49] M. Wimmer, M.-A. Miri, D. Christodoulides, and U. Peschel, *Sci. Rep.* **5**, 17760 (2015).
- [50] J. Zak, *Phys. Rev. B* **38**, 6322 (1988).
- [51] E. E. Mendez, F. Agulló-Rueda, and J. M. Hong, *Phys. Rev. Lett.* **60**, 2426 (1988).